Time Evolution of the Kondo Resonance in Response to a Quench

H. T. M. Nghiem[1,2] and T. A. Costi[1]
[1]Peter Grünberg Institut and Institute for Advanced Simulation, Research Centre Jülich, 52425 Jülich, Germany
[2]Advanced Institute for Science and Technology, Hanoi University of Science and Technology, 10000 Hanoi, Vietnam
(Received 24 January 2017; revised manuscript received 17 July 2017; published 13 October 2017)

We investigate the time evolution of the Kondo resonance in response to a quench by applying the time-dependent numerical renormalization group (TDNRG) approach to the Anderson impurity model in the strong correlation limit. For this purpose, we derive within the TDNRG approach a numerically tractable expression for the retarded two-time nonequilibrium Green function $G(t+t',t)$, and its associated time-dependent spectral function, $A(\omega,t)$, for times t both before and after the quench. Quenches from both mixed valence and Kondo correlated initial states to Kondo correlated final states are considered. For both cases, we find that the Kondo resonance in the zero temperature spectral function, a preformed version of which is evident at very short times $t \to 0^+$, only fully develops at very long times $t \gtrsim 1/T_K$, where T_K is the Kondo temperature of the final state. In contrast, the final state satellite peaks develop on a fast time scale $1/\Gamma$ during the time interval $-1/\Gamma \lesssim t \lesssim +1/\Gamma$, where Γ is the hybridization strength. Initial and final state spectral functions are recovered in the limits $t \to -\infty$ and $t \to +\infty$, respectively. Our formulation of two-time nonequilibrium Green functions within the TDNRG approach provides a first step towards using this method as an impurity solver within nonequilibrium dynamical mean field theory.

DOI: 10.1103/PhysRevLett.119.156601

Introduction.—The nonequilibrium properties of strongly correlated quantum impurity models continue to pose a major theoretical challenge. This contrasts with their equilibrium properties, which are largely well understood [1], or can be investigated within a number of highly accurate methods, such as the numerical renormalization group (NRG) method [2–5], the continuous time quantum Monte Carlo (CTQMC) approach [6], the density matrix renormalization group [7], or the Bethe ansatz method [8,9]. Quantum impurity models far from equilibrium are of direct relevance to several fields of research, including charge transfer effects in low-energy ion-surface scattering [10–17], transient and steady state effects in molecular and semiconductor quantum dots [18–36], and also in the context of dynamical mean field theory (DMFT) of strongly correlated lattice models [37–39], as generalized to nonequilibrium [40–42]. In the latter, further progress hinges on an accurate nonperturbative solution for the nonequilibrium Green functions of an effective quantum impurity model. Such a solution, beyond allowing time-resolved spectroscopies of correlated lattice systems within DMFT to be addressed [43–47], would also be useful in understanding time-resolved scanning tunnelling microscopy of nanoscale systems [48] and proposed cold atom realizations of Kondo correlated states [49–52], which could be probed with real-time radio-frequency spectroscopy [53–55].

In this Letter, we use the time-dependent numerical renormalization group (TDNRG) approach [56–62] to calculate the retarded two-time Green function, $G(t_1=t+t',t_2=t)$, and associated spectral function, $A(\omega,t)$, of the Anderson impurity model in response to a quench at time $t=0$, and apply this to investigate in detail the time evolution of the Kondo resonance. This topic has been addressed before within several approaches, including the noncrossing approximation [26,63], conserving approximations [64], and within the CTQMC method for quantum dots out of equilibrium [32]. Related work on the temporal evolution of the spin-spin correlation function in the Kondo model and thermalization in the Anderson impurity model following initial state preparations has also been carried out [65,66]. Formulations of the time-dependent spectral function within the TDNRG approach are also available [59,67], but only for positive times. Here, we derive expressions for the two-time Green function and spectral function $A(\omega,t)$ which are numerically tractable at arbitrary times, including negative times. The main advantages of the TDNRG approach over other approaches for calculating time-dependent spectral functions is that it can access arbitrary long times ($t \to \pm\infty$) and arbitrary low temperatures and frequencies, is nonperturbative and calculates spectral functions directly on the real frequency axis. It is therefore well suited for investigating the formation in time of the exponentially narrow and low temperature Kondo resonance [68].

Model and quenches.—We consider the time-dependent Anderson impurity model, $H=\sum_\sigma \varepsilon_d(t) n_{d\sigma} + U(t) n_{d\uparrow} n_{d\downarrow} + \sum_{k\sigma} \epsilon_k c^\dagger_{k\sigma} c_{k\sigma} + \sum_{k\sigma} V(c^\dagger_{k\sigma} d_\sigma + d^\dagger_\sigma c_{k\sigma})$, where $\varepsilon_d(t) = \theta(-t)\varepsilon_i + \theta(t)\varepsilon_f$ is the energy of the local level, $U(t) = \theta(-t)U_i + \theta(t)U_f$ is the local Coulomb interaction, σ labels the spin, $n_{d\sigma} = d^\dagger_\sigma d_\sigma$ is the number operator for local electrons with spin σ, and ϵ_k is the kinetic energy of the conduction electrons with constant density of states $\rho(\omega)=\sum_k \delta(\omega-\epsilon_k)=1/2D$ with $D=1$ the half-bandwidth.

We take $\Gamma \equiv \pi\rho(0)V^2 = 0.001$ throughout and consider two types of quench [referred to subsequently as quench (A) or quench (B)]: (A), from a symmetric Kondo regime with $\varepsilon_i = -15\Gamma$, $U_i = 30\Gamma$ and a vanishingly small Kondo scale $T_K^i = 3 \times 10^{-8}$ [71] to a symmetric Kondo regime with $\varepsilon_f = -6\Gamma$, $U_f = 12\Gamma$ and a larger Kondo scale $T_K = 2.5 \times 10^{-5}$, and, (B), from a mixed valence regime with $\varepsilon_i = -\Gamma$, $U_i = 8\Gamma$ to a symmetric Kondo regime with $\varepsilon_f = -4\Gamma$, $U_f = 8\Gamma$ and a Kondo scale $T_K = 1.0 \times 10^{-4}$.

Spectral function $A(\omega, t)$.—We obtain the time-dependent spectral function via $A(\omega, t) = -(1/\pi)\mathrm{Im}[G(\omega + i\eta, t)]$, where $G(\omega + i\eta, t)$, with infinitesimal $\eta > 0$, is the Fourier transform of $G(t + t', t) \equiv -i\theta(t')\langle [d_\sigma(t + t'), d_\sigma^\dagger(t)]_+ \rangle_{\hat{\rho}}$ with respect to the relative time t' and $\hat{\rho}$ denotes the full density matrix of the initial state [73–75]. In the notation of Ref. [61], we find for the case of positive times [76]

$$G(\omega + i\eta, t) = \sum_{m=m_0}^{N} \sum_{rsq}^{\notin KK'K''} \rho_{sr}^{i\to f}(m) e^{-i(E_s^m - E_r^m)t} \times \left(\frac{B_{rq}^m C_{qs}^m}{\omega + E_r^m - E_q^m + i\eta} + \frac{C_{rq}^m B_{qs}^m}{\omega + E_q^m - E_s^m + i\eta} \right), \quad (1)$$

where $B = d_\sigma$, $C = d_\sigma^\dagger$, and $\rho_{sr}^{i\to f}(m) = \sum_{ef} \langle sem|\hat{\rho}|rem\rangle_f$ is the full reduced density matrix projected onto the final states [61]. A somewhat more complicated expression can be derived for negative times [76]. From Eq. (1), we see that the spectral function can be calculated highly efficiently at all times and frequencies from a knowledge of $\rho_{sr}^{i\to f}(m)$, the final state matrix elements, and excitations at each shell m. Our expressions for $A(\omega, t)$ in the two time domains $t < 0$ and $t > 0$ recover the initial and final state spectral functions for $t \to -\infty$ and $t \to +\infty$, respectively, and satisfy the spectral sum rule $\int_{-\infty}^{+\infty} d\omega A(\omega, t) = 1$ exactly [76]. Below, we shall first focus on positive times, where the main time evolution of the Kondo resonance occurs, then on negative to positive times, showing how the high energy final state features in $A(\omega, t)$ evolve from their initial state counterparts already at negative times.

Results for positive times.—Consider quench (A), i.e., switching between symmetric Kondo regimes with $T_K^i \ll T_K$. Figure 1(a) shows the overall time dependence of the spectral function $A(\omega > 0, t > 0) = A(-\omega, t > 0)$. Two structures, associated with two energy scales, are visible at all times $t > 0$: the satellite peak at $\omega = \varepsilon_f + U_f \approx 240 T_K$ and a structure on the scale of T_K around the Fermi level. The former has negligible time dependence, indicating that the satellite peak in the spectral function has already formed by time $t = 0$ (its evolution at negative times from the initial state satellite peak at $\omega = \varepsilon_i + U_i > \varepsilon_f + U_f$ is discussed below). In contrast to this, the structure around the Fermi level has significant time dependence at $t > 0$ and evolves into the fully formed final state Kondo resonance only on time scales $t \gtrsim 1/T_K$ [Figs. 1(c) and 1(d)] in agreement with Ref. [26] for the $U = \infty$ Anderson model. For $tT_K \gg 1$, the height of the Kondo resonance at the Fermi level approaches its unitary value given by the Friedel sum rule $\pi\Gamma A(\omega = 0, t \to \infty) = 1$ to within 15% [Fig. 1(d)]. The small deviation from the expected value is a result of incomplete thermalization due to the discretized Wilson chain used within the TDNRG approach [67,69,76]. Consequently, evaluating $A(\omega, t \to \infty)$ via the self-energy [80] does not improve the Friedel sum rule further in this limit [59]. In the opposite limit, $t \to -\infty$, where thermalization is not an issue, we recover the Friedel sum rule to within 3% (discussed below). The use of a discrete Wilson chain is also the origin of the small substructures at $|\omega| \lesssim T_K$ in Figs. 1(b)–1(d), effects seen in the time evolution of other quantities, such as the local occupation, and explained in terms of the discrete Wilson chain [81]. On shorter time scales, $tT_K \lesssim 1$, states in the region $T_K^i \ll |\omega| < T_K$, initially missing [Fig. 1(b)], are gradually filled in by a transfer of spectral weight from higher energies [Fig. 1(c)] to form the final state Kondo resonance at long times [Fig. 1(d)]. The presence of a structure on the final state Kondo scale T_K at short times $t \to 0^+$ is understood as follows: the Fourier transform with

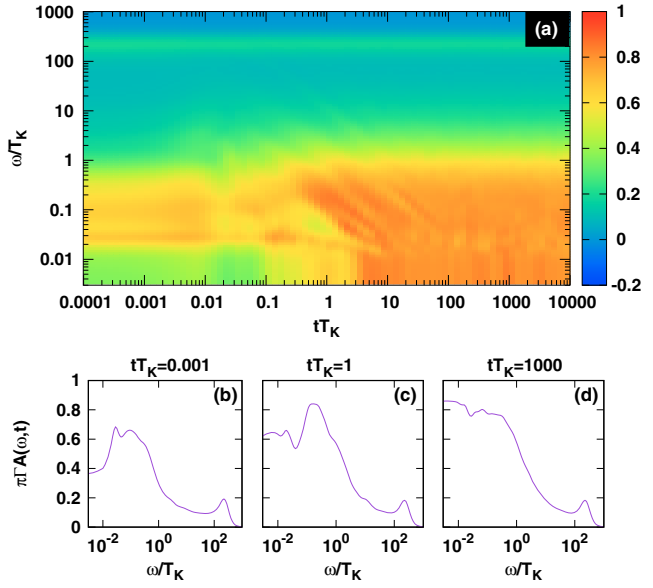

FIG. 1. (a) Time evolution of the normalized spectral function $\pi\Gamma A(\omega > 0, t)$ for the symmetric Anderson model at positive times, following a quench at $t = 0$ specified by $\varepsilon_i = -15\Gamma$, $U_i = 30\Gamma$, and $\varepsilon_f = -6\Gamma$, $U_f = 12\Gamma$ with final state Kondo temperature $T_K = 2.5 \times 10^{-5}$. A structure on the scale of T_K evolves into the Kondo resonance at long times $t \gtrsim 1/T_K$, while a structure at $\omega = \varepsilon_f + U_f \approx 240 T_K$ with negligible time dependence corresponds to the final state satellite peak. Panels (b)–(d) show the spectral function at times $tT_K = 0.001$, 1, and 1000, respectively. The TDNRG calculations used a discretization parameter $\Lambda = 4$, z averaging [78,79] with $N_z = 32$ and a cutoff energy $E_{\mathrm{cut}} = 24$.

respect to $t' = t_1 - t_2$ necessarily convolutes information about the final state at large t_1, t_2 into the spectral function at short times t [82]. Hence, the gross features of the spectral function, even at short times $t \to 0^+$, are close to those of the final state spectral function $A(\omega, t \to \infty)$, and far from those of the initial state spectral function. Clear signatures of the latter, such as the much narrower initial state Kondo peak, only appear at negative times.

Consider now quench (B), in which the system, is switched from the mixed valence to the symmetric Kondo regime. Figures 2(a) and 2(b) show the overall time dependence of the spectral function for $\omega < 0$ [Fig. 2(a)] and $\omega > 0$ [Fig. 2(b)]. As for quench (A), two structures associated with two energy scales are again visible at all times $t > 0$: the satellite peaks at $\omega = \varepsilon_f \approx -40T_K$ [Fig. 2(a)] and $\omega = \varepsilon_f + U \approx +40T_K$ [Fig. 2(b)] and a structure on the scale of T_K around the Fermi level [Figs. 2(a) and 2(b)]. In contrast to quench (A), the former have some non-negligible time dependence at short positive times as can be seen in Fig. 2(c) for $tT_K = 10^{-4}$ ($t\Gamma = 10^{-3}$), where the weight of the satellite peaks has still not equalized. This asymmetry vanishes on time scales exceeding $1/\Gamma$ [Figs. 2(d) and 2(e) for $tT_K = 1$ ($t\Gamma = 10$) and $tT_K = 10^4$ ($t\Gamma = 10^3$), respectively]. The low energy structure of width T_K, initially asymmetric and exceeding the unitary height $1/\pi\Gamma$, has significant time dependence for $t > 0$ and evolves into the fully developed Kondo resonance at $t \gtrsim 1/T_K$ [Figs. 2(d) and 2(e)]. The deviation from the Friedel sum rule $\pi\Gamma A(\omega = 0, t \to \infty) = 1$ is comparable to that for quench (A) and reflects the incomplete thermalization due to the discrete Wilson chain used within the TDNRG approach. The discrete Wilson chain also results in the substructures at $|\omega| \lesssim T_K$ in Figs. 2(c) and 2(d) and in the small remaining asymmetry of the fully developed Kondo resonance in Fig. 2(e).

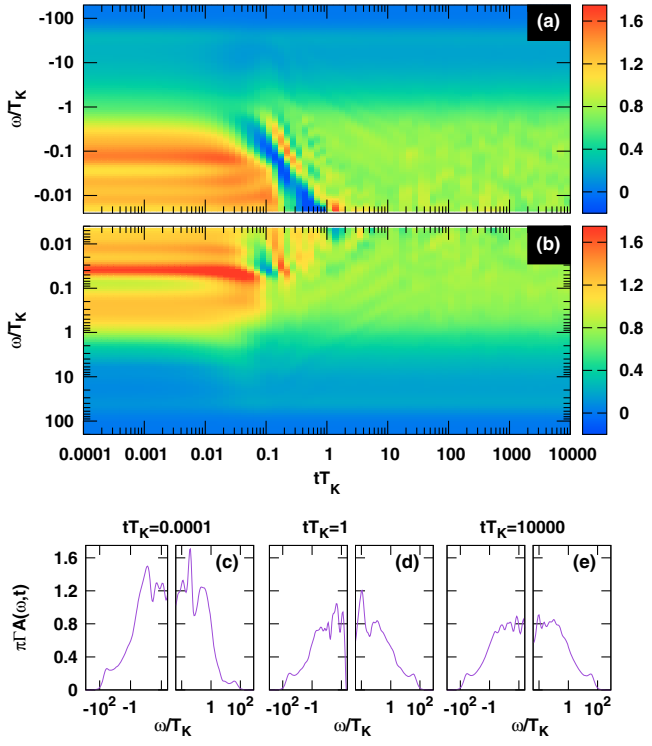

FIG. 2. Time evolution of the normalized spectral function $\pi\Gamma A(\omega, t)$ at positive times, for, (a), negative, and, (b), positive frequencies, for quench (A) from the mixed valence to the symmetric Kondo regime with $T_K = 1.0 \times 10^{-4}$. A structure on the scale of T_K evolves into the Kondo resonance at long times $t \gtrsim 1/T_K$, while structures at $\omega = \pm\varepsilon_f \approx \pm 40T_K$, with negligible time-dependence, correspond to the final state satellite peaks. Panels (c)–(e) show the spectral function at times $tT_K = 0.0001$, 1, and 10000, respectively. TDNRG parameters: $\Lambda = 4$, z averaging with $N_z = 64$ and a cutoff energy $E_{\text{cut}} = 24$.

From negative to positive times.—Figures 3(a) and 3(b) show the overall time dependence of the spectral function for negative and positive times, respectively, for quench (A), on a *linear* frequency scale. As for positive times [Fig. 1(a) and Fig. 3(b)], low and high energy structures are visible also for negative times [Fig. 3(a)]. Moreover, it is clear from Figs. 3(a) and 3(b) that the transition from the initial to the final state spectral function occurs on different time scales for the different structures. Consider first the high energy structures, which carry essentially all the spectral weight. Initially, these are located at $\omega = \pm\varepsilon_i \approx \pm 600T_K$ as is clearly visible in Fig. 3(a) or in Fig. 3(c) for $tT_K = -10^3$ ($t\Gamma = -4 \times 10^4 \ll -1$). They cross over to their final state positions at $\omega = \pm\varepsilon_f = \pm 240T_K$ when $tT_K \gtrsim -10^{-2}$

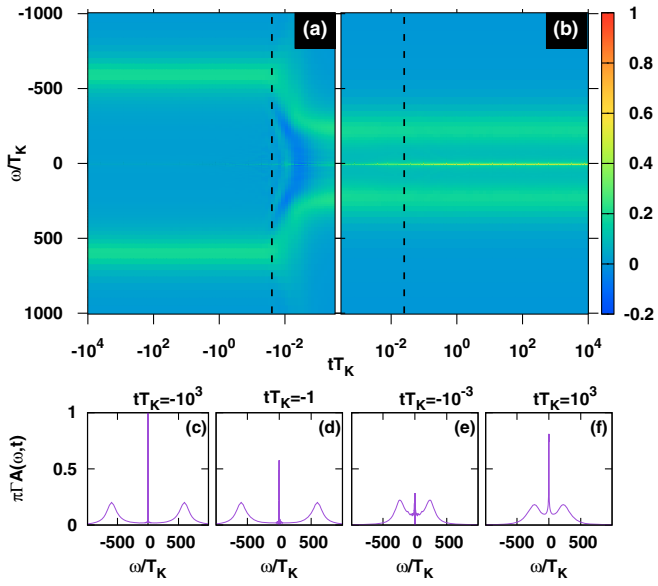

FIG. 3. $A(\omega, t)$ vs tT_K from, (a), negative, to, (b), positive times for quench (A), and on a *linear* frequency scale. Dashed lines mark $t\Gamma = \pm 1$ ($tT_K = \pm 2.5 \times 10^{-2}$). Initial state ($\omega = \pm\varepsilon_i = \pm 15\Gamma \approx \pm 600T_K$) and final state ($\omega = \pm\varepsilon_f = \pm 6\Gamma \approx \pm 240T_K$) satellite peaks are clearly visible, as are initial and final state Kondo resonances around $\omega = 0$. Panels (c)–(f) show the $A(\omega, t)$ at times $tT_K = -1000, -1, -0.001$, and $+1000$, respectively. TDNRG parameters as in Fig. 2.

($t\Gamma \gtrsim -0.4$) [Figs. 3(a) and 3(e)], i.e., on the charge fluctuation time scale $1/\Gamma$. This can also be seen in Figs. 3(d) and 3(e). This large shift in spectral weight from $\omega = \pm\varepsilon_i$ to $\omega = \pm\varepsilon_f$ in the time range $-10^{-2} \lesssim tT_K \lesssim -10^{-3}$ ($-0.4 \lesssim t\Gamma \lesssim -0.04$), clearly seen in Fig. 3(a), is accompanied by small regions of negative spectral weight in this transient time range [76]. This does not violate any exact results for time-dependent, as opposed to steady-state, spectral functions, and is observed in other systems [30,83,84]. The spectral sum rule is satisfied analytically exactly at all times and numerically within 1% at all negative times and to higher accuracy at positive times for all quench protocols [76]. Turning now to the low energy structure, i.e., the Kondo resonance, the use of a linear frequency scale now allows the initial state Kondo resonance at $\omega = 0$ to be clearly seen in Fig. 3(a) [see also Fig. 3(c)]. This structure, of width $T_K^i \ll T_K$ at $t \to -\infty$ and satisfying the Friedel sum rule $\pi\Gamma A(\omega=0, t\to-\infty)=1$, gradually broadens and acquires a width of T_K at short negative times [76], and then evolves into the fully developed Kondo resonance on positive time scales $tT_K \gtrsim 1$ [Fig. 3(e)].

Even more interesting is the negative [Fig. 4(a)] to positive [Fig. 4(b)] time evolution of the spectral function upon quenching from the mixed valence to the symmetric Kondo regime [quench (B)]. At large negative times [Fig. 4(c)], one recovers the initial state spectral function of the mixed valence regime (with $\varepsilon_i = -\Gamma$) showing a mixed valence resonance, renormalized by many-body effects to lie close to, but just above the Fermi level

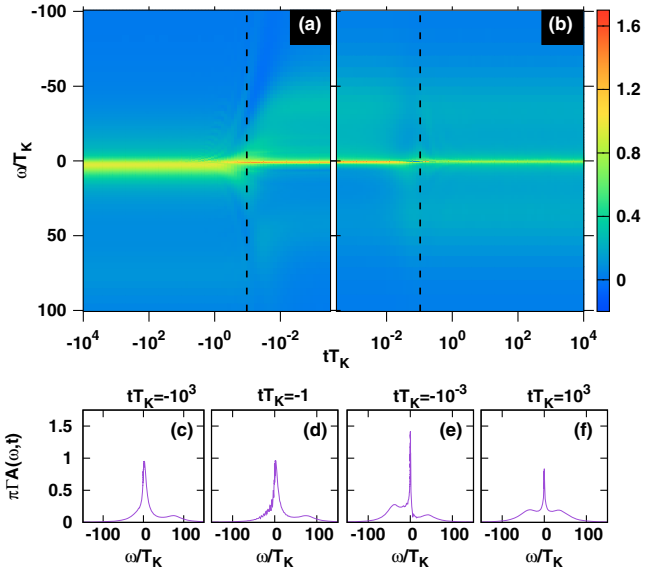

FIG. 4. $A(\omega, t)$ vs tT_K from, (a), negative, to, (b), positive times and on a *linear* frequency scale for quench (B) (from a mixed valence to a symmetric Kondo regime). Dashed lines mark $t\Gamma = \pm 1$ ($tT_K = \pm 10^{-1}$). Panels (c)–(f) show the spectral function at times $tT_K = -1000, -1, -0.001$, and $+1000$, respectively. TDNRG parameters as in Fig. 2.

$\varepsilon_i \to \tilde{\varepsilon}_i \gtrsim 0$ and satisfying the Friedel sum rule $A(0, t\to-\infty) = \sin^2(\pi n_d/2)/\pi\Gamma$ to within 3% [85] [Figs. 4(a) and 4(c), $n_d = 0.675$]. The upper satellite peak at $\omega = \varepsilon_i + U_i = 7\Gamma \approx 70T_K$ is more clearly visible in Fig. 4(c). These peaks give rise to the final state satellite peaks at $\omega = \pm\varepsilon_f = \pm 4\Gamma \approx \pm 40T_K$ which start to form already at negative times $tT_K \gtrsim -10^{-1}$ ($t\Gamma \gtrsim -1$), i.e., on the charge fluctuation time scale $1/\Gamma$, as for quench (A). While the positions of these peaks start to shift to their final state values at negative times $tT_K \gtrsim -10^{-1}$ ($t\Gamma \gtrsim -1$), their weights remain disparate [see Fig. 4(e)] and only equalize at $tT_K \gtrsim +10^{-1}$ ($t\Gamma \gtrsim +1$) as clearly seen in Fig. 4(b); i.e., the formation of the high energy final state satellite peaks occurs on a fast time scale $t \approx 1/\Gamma$ in the interval $-1/\Gamma \lesssim t \lesssim +1/\Gamma$ (dashed lines in Fig. 4). Going into more details, we see in Figs. 4(a) and 4(c)–4(e) the deconstruction of the mixed valence resonance in the time range $-1/\Gamma < t < 0$. While this resonance carries essentially all the spectral weight at $t \ll -1/\Gamma$, weight is gradually transferred to $\omega < 0$, with precursor oscillations starting at $tT_K = -1$ ($t\Gamma = -10$) [Fig. 4(d)], to form the lower final state satellite peak at $\omega = \varepsilon_f$ for $-1/\Gamma < t < 0$ [Fig. 4(e)]. Simultaneously, the mixed valence resonance narrows from its original width $\Gamma \approx 10T_K$ and shifts towards the Fermi level to form a low energy structure on the scale of T_K [Fig. 4(e)]. The latter eventually evolves into the final state Kondo resonance at $tT_K \gtrsim 1$. The final state spectral function is recovered in the long-time limit $tT_K \gg 1$ [Fig. 4(f)].

Conclusions.—In summary, we investigated within the TDNRG approach, the time evolution of the spectral function of the Anderson impurity model in the strong correlation limit. Quenching into a Kondo correlated final state, we showed that the Kondo resonance in the zero temperature spectral function only fully develops at very long times $t \gtrsim 1/T_K$, although a preformed version of it is evident even at very short times $t \to 0^+$. The latter can be used as a smoking gun signature of the transient build up of the Kondo resonance in future cold atom realizations of the Anderson impurity model [50]. The satellite peaks evolve from their initial state values at negative times on a much faster time scale $t \approx 1/\Gamma$ in the time-interval $-1/\Gamma \lesssim t \lesssim 1/\Gamma$. Our formulation of sum rule conserving two-time nonequilibrium Green functions within the TDNRG approach, including lesser Green functions, and their explicit dependence on both times [76], yields the basic information required for applications to time-dependent quantum transport [30] and constitutes a first step towards using the TDNRG approach as an impurity solver within nonequilibrium DMFT [41,42,86].

H. T. M. N. thanks Hung T. Dang for fruitful discussions. We acknowledge support from the Deutsche Forschungsgemeinschaft via RTG 1995 and supercomputer support by the John von Neumann institute for Computing (Jülich). One of the authors (T. A. C.) acknowledges useful discussions with A. Rosch, J. K. Freericks, and the

hospitality of the Aspen Center for Physics, supported by the National Science Foundation under Grant No. PHY-1607611, during completion of this work.

[1] A. C. Hewson, Phys. Rev. Lett. **70**, 4007 (1993).
[2] K. G. Wilson, Rev. Mod. Phys. **47**, 773 (1975).
[3] H. R. Krishna-murthy, J. W. Wilkins, and K. G. Wilson, Phys. Rev. B **21**, 1003 (1980).
[4] R. Bulla, T. A. Costi, and T. Pruschke, Rev. Mod. Phys. **80**, 395 (2008).
[5] C. Gonzalez-Buxton and K. Ingersent, Phys. Rev. B **57**, 14254 (1998).
[6] E. Gull, A. J. Millis, A. I. Lichtenstein, A. N. Rubtsov, M. Troyer, and P. Werner, Rev. Mod. Phys. **83**, 349 (2011).
[7] S. R. White, Phys. Rev. Lett. **69**, 2863 (1992).
[8] A. M. Tsvelick and P. B. Wiegmann, Adv. Phys. **32**, 453 (1983).
[9] N. Andrei, in *Low-Dimensional Quantum Field Theories for Condensed Matter Physicists* (World Scientific Publishing Co, Singapore, 2013), pp. 457–551.
[10] R. Brako and D. Newns, Surf. Sci. **108**, 253 (1981).
[11] H. Kasai and A. Okiji, Surf. Sci. **183**, 147 (1987).
[12] J. Merino and J. B. Marston, Phys. Rev. B **58**, 6982 (1998).
[13] D. C. Langreth and P. Nordlander, Phys. Rev. B **43**, 2541 (1991).
[14] H. Shao, D. C. Langreth, and P. Nordlander, Phys. Rev. B **49**, 13929 (1994).
[15] H. Shao, D. C. Langreth, and P. Nordlander, Phys. Rev. B **49**, 13948 (1994).
[16] M. Pamperin, F. X. Bronold, and H. Fehske, Phys. Rev. B **91**, 035440 (2015).
[17] X. He and J. A. Yarmoff, Phys. Rev. Lett. **105**, 176806 (2010).
[18] S. Hershfield, J. H. Davies, and J. W. Wilkins, Phys. Rev. B **46**, 7046 (1992).
[19] S. Hershfield, Phys. Rev. Lett. **70**, 2134 (1993).
[20] Y. Meir, N. S. Wingreen, and P. A. Lee, Phys. Rev. Lett. **70**, 2601 (1993).
[21] C. Bruder and H. Schoeller, Phys. Rev. Lett. **72**, 1076 (1994).
[22] A. V. Kretinin, H. Shtrikman, D. Goldhaber-Gordon, M. Hanl, A. Weichselbaum, J. von Delft, T. Costi, and D. Mahalu, Phys. Rev. B **84**, 245316 (2011).
[23] A. V. Kretinin, H. Shtrikman, and D. Mahalu, Phys. Rev. B **85**, 201301 (2012).
[24] M. Pletyukhov and H. Schoeller, Phys. Rev. Lett. **108**, 260601 (2012).
[25] G. D. Scott, D. Natelson, S. Kirchner, and E. Muñoz, Phys. Rev. B **87**, 241104 (2013).
[26] P. Nordlander, M. Pustilnik, Y. Meir, N. S. Wingreen, and D. C. Langreth, Phys. Rev. Lett. **83**, 808 (1999).
[27] J. Park, A. Pasupathy, J. Goldsmith, C. Chang, Y. Yaish, J. Petta, M. Rinkoski, J. Sethna, H. Abruna, P. McEuen, and D. Ralph, Nature (London) **417**, 722 (2002).
[28] A. Kogan, S. Amasha, and M. A. Kastner, Science **304**, 1293 (2004).
[29] B. Hemingway, S. Herbert, M. Melloch, and A. Kogan, Phys. Rev. B **90**, 125151 (2014).
[30] A.-P. Jauho, N. S. Wingreen, and Y. Meir, Phys. Rev. B **50**, 5528 (1994).
[31] D. M. Kennes, S. G. Jakobs, C. Karrasch, and V. Meden, Phys. Rev. B **85**, 085113 (2012).
[32] G. Cohen, E. Gull, D. R. Reichman, and A. J. Millis, Phys. Rev. Lett. **112**, 146802 (2014).
[33] T. L. Schmidt, P. Werner, L. Mühlbacher, and A. Komnik, Phys. Rev. B **78**, 235110 (2008).
[34] A. Dorda, M. Nuss, W. von der Linden, and E. Arrigoni, Phys. Rev. B **89**, 165105 (2014).
[35] A. Rosch, J. Paaske, J. Kroha, and P. Wölfle, Phys. Rev. Lett. **90**, 076804 (2003).
[36] A. E. Antipov, Q. Dong, and E. Gull, Phys. Rev. Lett. **116**, 036801 (2016).
[37] W. Metzner and D. Vollhardt, Phys. Rev. Lett. **62**, 324 (1989).
[38] A. Georges, G. Kotliar, W. Krauth, and M. J. Rozenberg, Rev. Mod. Phys. **68**, 13 (1996).
[39] G. Kotliar and D. Vollhardt, Phys. Today **57**, 53 (2004).
[40] P. Schmidt and H. Monien, arXiv:cond-mat/0202046.
[41] J. K. Freericks, V. M. Turkowski, and V. Zlatić, Phys. Rev. Lett. **97**, 266408 (2006).
[42] H. Aoki, N. Tsuji, M. Eckstein, M. Kollar, T. Oka, and P. Werner, Rev. Mod. Phys. **86**, 779 (2014).
[43] M. Eckstein and M. Kollar, Phys. Rev. B **78**, 205119 (2008).
[44] J. K. Freericks, H. R. Krishnamurthy, and T. Pruschke, Phys. Rev. Lett. **102**, 136401 (2009).
[45] L. Perfetti, P. A. Loukakos, M. Lisowski, U. Bovensiepen, H. Berger, S. Biermann, P. S. Cornaglia, A. Georges, and M. Wolf, Phys. Rev. Lett. **97**, 067402 (2006).
[46] P. A. Loukakos, M. Lisowski, G. Bihlmayer, S. Blügel, M. Wolf, and U. Bovensiepen, Phys. Rev. Lett. **98**, 097401 (2007).
[47] E. Iyoda and S. Ishihara, Phys. Rev. B **89**, 125126 (2014).
[48] S. Loth, M. Etzkorn, C. P. Lutz, D. M. Eigler, and A. J. Heinrich, Science **329**, 1628 (2010).
[49] Y. Nishida, Phys. Rev. Lett. **111**, 135301 (2013).
[50] J. Bauer, C. Salomon, and E. Demler, Phys. Rev. Lett. **111**, 215304 (2013).
[51] Y. Nishida, Phys. Rev. A **93**, 011606 (2016).
[52] L. Riegger, N. Darkwah Oppong, M. Höfer, D. Rio Fernandes, I. Bloch, and S. Fölling, arXiv:1708.03810.
[53] J. Goold, T. Fogarty, N. Lo Gullo, M. Paternostro, and T. Busch, Phys. Rev. A **84**, 063632 (2011).
[54] M. Knap, A. Shashi, Y. Nishida, A. Imambekov, D. A. Abanin, and E. Demler, Phys. Rev. X **2**, 041020 (2012).
[55] M. Cetina, M. Jag, R. S. Lous, I. Fritsche, J. T. M. Walraven, R. Grimm, J. Levinsen, M. M. Parish, R. Schmidt, M. Knap, and E. Demler, Science **354**, 96 (2016).
[56] F. B. Anders and A. Schiller, Phys. Rev. Lett. **95**, 196801 (2005).
[57] F. B. Anders and A. Schiller, Phys. Rev. B **74**, 245113 (2006).
[58] F. B. Anders, Phys. Rev. Lett. **101**, 066804 (2008).
[59] F. B. Anders, J. Phys. Condens. Matter **20**, 195216 (2008).
[60] F. Güttge, F. B. Anders, U. Schollwöck, E. Eidelstein, and A. Schiller, Phys. Rev. B **87**, 115115 (2013).
[61] H. T. M. Nghiem and T. A. Costi, Phys. Rev. B **89**, 075118 (2014).

[62] H. T. M. Nghiem and T. A. Costi, Phys. Rev. B **90**, 035129 (2014).
[63] F. Randi, D. Fausti, and M. Eckstein, Phys. Rev. B **95**, 115132 (2017).
[64] S. Bock, A. Liluashvili, and T. Gasenzer, Phys. Rev. B **94**, 045108 (2016).
[65] D. Lobaskin and S. Kehrein, Phys. Rev. B **71**, 193303 (2005).
[66] M. Heyl and S. Kehrein, Phys. Rev. B **81**, 144301 (2010).
[67] I. Weymann, J. von Delft, and A. Weichselbaum, Phys. Rev. B **92**, 155435 (2015).
[68] The use of a discretized Wilson chain within the TDNRG approach results, to a small degree, in incomplete thermalization at $t \to \infty$ in thermodynamic observables [57,61,69,70], and in spectral functions [59,67], but it suffices for a consistent nonperturbative picture of the overall time evolution of $A(\omega, t)$.
[69] A. Rosch, Eur. Phys. J. B **85**, 6 (2012).
[70] H. T. M. Nghiem, D. M. Kennes, C. Klöckner, V. Meden, and T. A. Costi, Phys. Rev. B **93**, 165130 (2016).
[71] We use the Bethe ansatz expression $T_K = \sqrt{\Gamma U/2} e^{-\pi U/8\Gamma + \pi\Gamma/2U}$ valid in the symmetric Kondo limit $U/\pi\Gamma \gg 1$ [1,72].
[72] V. Zlatić and B. Horvatić, Phys. Rev. B **28**, 6904 (1983).
[73] A. Weichselbaum and J. von Delft, Phys. Rev. Lett. **99**, 076402 (2007).
[74] R. Peters, T. Pruschke, and F. B. Anders, Phys. Rev. B **74**, 245114 (2006).
[75] T. A. Costi and V. Zlatić, Phys. Rev. B **81**, 235127 (2010).
[76] See Supplemental Material at http://link.aps.org/supplemental/10.1103/PhysRevLett.119.156601 for derivations and additional results, including Ref. [77].
[77] R. Bulla, T. A. Costi, and D. Vollhardt, Phys. Rev. B **64**, 045103 (2001).
[78] W. C. Oliveira and L. N. Oliveira, Phys. Rev. B **49**, 11986 (1994).
[79] V. L. Campo and L. N. Oliveira, Phys. Rev. B **72**, 104432 (2005).
[80] R. Bulla, A. C. Hewson, and T. Pruschke, J. Phys. Condens. Matter **10**, 8365 (1998).
[81] E. Eidelstein, A. Schiller, F. Güttge, and F. B. Anders, Phys. Rev. B **85**, 075118 (2012).
[82] V. Turkowski and J. K. Freericks, Phys. Rev. B **71**, 085104 (2005).
[83] A. Dirks, M. Eckstein, T. Pruschke, and P. Werner, Phys. Rev. E **87**, 023305 (2013).
[84] J. K. Freericks and V. Turkowski, Phys. Rev. B **80**, 115119 (2009).
[85] T. A. Costi, J. Kroha, and P. Wölfle, Phys. Rev. B **53**, 1850 (1996).
[86] C. Gramsch, K. Balzer, M. Eckstein, and M. Kollar, Phys. Rev. B **88**, 235106 (2013).